Termination dependence of surface stacking at 4*H*-SiC(0001)-1×1: Density functional theory calculations

Hideyuki Hara,[1,*] Yoshitada Morikawa,[2,†] Yasuhisa Sano,[1] and Kazuto Yamauchi[1,3]

[1]*Department of Precision Science and Technology, Graduate School of Engineering, Osaka University, 2-1, Yamada-oka, Suita, Osaka 565-0871, Japan*

[2]*The Institute of Scientific and Industrial Research (ISIR), Osaka University, 8-1, Mihogaoka, Ibaraki, Osaka 567-0047, Japan*

[3]*Research Center for Ultra-Precision Science and Technology, Graduate School of Engineering, Osaka University, 2-1, Yamada-oka, Suita, Osaka 565-0871, Japan*

(Received 30 October 2008; revised manuscript received 25 March 2009; published 27 April 2009)

We study the effect of adsorbates on the relative stability of hexagonal and cubic stacking sequences at the topmost SiC bilayers of 4*H*-SiC(0001)-1×1 surfaces using first-principles calculations. We investigate F-terminated, OH-terminated, H-terminated, and clean surfaces, and in all cases, the cubic structure is more stable than the hexagonal structure. The energy difference between the two structures, however, significantly depends on adsorbates and is largest on the clean surface while it is smallest on the H-terminated surface. Stabilization of the cubic structure at F-terminated and OH-terminated surfaces is in contradiction to a simple argument based on the electrostatic interaction and we attribute it to orbital hybridization between occupied states of adsorbates and unoccupied states of the substrate surface. The present results suggest a possible means of controlling step bunching and the SiC stacking sequence by surface adsorbates.

DOI: 10.1103/PhysRevB.79.153306 PACS number(s): 65.40.gp

Silicon carbide (SiC) is a unique compound semiconductor that possesses a number of tetrahedral polytypes. 4*H* and 6*H*-SiC polytypes are promising materials for high-power electronics[1] and III–V nitride substrates.[2] They have both cubic zinc-blende (*ABC* stacking sequence) and hexagonal wurtzite (*ABA* stacking sequence) structures of SiC bilayers whose existence cause both fundamental problems and interesting properties.

High-temperature processes using gas etching,[3–8] sublimation growth,[9] and chemical-vapor deposition[10] produce step bunching or step faceting of 4*H* and 6*H*-SiC surfaces. In SiC metal-oxide-semiconductor field-effect transistors, the roughening of the interface due to step bunching deteriorates the channel mobility. Recently, flat surfaces without step bunching have been achieved using electronless wet etching.[11–13] The wet-etched surface had alternating narrow and broad terraces, which correspond to two different stacking structures on the 4*H*-SiC(0001)-1×1 surface.[12] The narrow and broad terraces were attributed to hexagonal and cubic structures at the two topmost SiC bilayers by considering the relative surface stability. The step-bunching mechanism has been discussed in terms of kinetics and surface energies.

Heine and co-workers[14,15] calculated the relative energies of several different polytypes of SiC crystal using a first-principles electronic structure method. They obtained interaction energies up to the third nearest-neighbor SiC bilayers for the generalized axial next-nearest-neighbor Ising (ANNNI) model and reported that the near degeneracy of polytypes comes from the relation $J_1 \simeq 1.89|J_2|$ with negative J_2. The generalized ANNNI model can be used not only to estimate the relative stability of bulk polytypes but also to account for the heteroepitaxial growth mode[16] and stacking faults[17] as well as the relative surface stability of step bunching.[6,10]

It is important to investigate the surface energetics to understand and control step bunching at SiC surfaces. In this paper, we examine the effects of termination on the relative stability of surface stacking by simulating F-terminated, OH-terminated, H-terminated, and clean 4*H*-SiC(0001)-1×1 surfaces from first principles. A clean 4*H*-SiC(0001)-1×1 surface was not observed experimentally but is included in our study for comparison.

We performed total-energy calculations and geometry optimizations based on the density functional theory[18,19] within a generalized gradient approximation of Perdew *et al.*[20] using a program package "STATE" (simulation tool for atom technology).[21] Vanderbilt's ultrasoft pseudopotentials[22] are used for C 2*p*, F 2*p*, and H 1*s* components while other components are described by the Troullier-Martins norm-conserving pseudopotentials.[23] Wave functions are expanded in a plane-wave basis set, and the cutoff energy for wave functions is 36 Ry and the cutoff for augmentation charges is 400 Ry. A 14×14 uniform mesh *k*-point set is used to

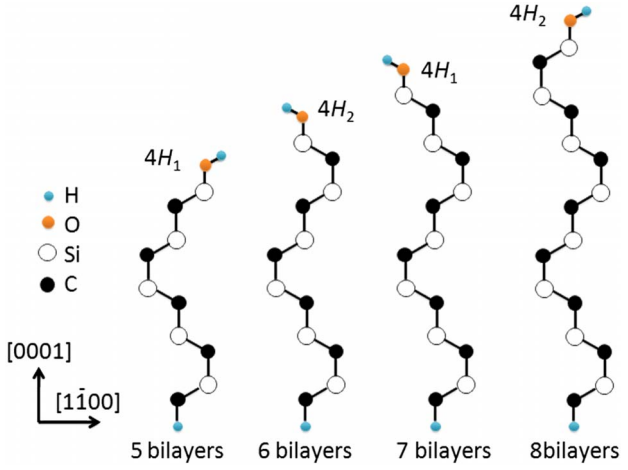

FIG. 1. (Color online) Atomic structure of OH-terminated 4*H*-SiC(0001)-1×1 surfaces. To clearly show the stacking sequences of SiC bilayers, only one unit cell of each SiC slab is shown. The bottom layer of the model slab is terminated by atomic H.

TABLE I. Lattice constants (a and c/na), total energy per SiC pair relative to the 6H structure (ΔE), and band gaps of 3C and $n$$H$-SiC structures.

	Method	a/nm	c/na	ΔE/meV	E_g/eV
6H	GGA-PBE[a]	0.3102	0.8175	0.0	2.04
	LDA	0.3062[b]	0.8172[b]	0.0[c]	1.96[d]
	GGA-PW91[e]	0.3044	0.8187	0.0	2.23
	Exp.	0.3081[f]	0.8178[f]		3.02[g]
4H	GGA-PBE[a]	0.3102	0.8182	0.21	2.23
	LDA	0.3061[b]	0.8179[b]	0.4[c]	2.18[d]
	GGA-PW91[e]	0.3043	0.8198	0.0	2.43
	Exp.	0.3081[f]	0.8184[f]		3.26[g]
3C	GGA-PBE[a]	0.4389		0.96	1.49
	LDA	0.4332[b]		1.2[c]	1.27[d]
	GGA-PW91[e]	0.4309		1.0	1.64
	Exp.[g]	0.4360			2.23
2H	GGA-PBE[a]	0.3100	0.8206	7.71	2.39
	LDA	0.3057[b]	0.8201[b]	9.9[c]	2.10[d]
	GGA-PW91[e]	0.3041	0.8219	7.9	2.54
	Exp.[g]	0.3076	0.8205		3.33

[a]Present study.
[b]Reference 28.
[c]Reference 14.
[d]Reference 27.
[e]Reference 30.
[f]Reference 24.
[g]Reference 25.

sample the surface Brillouin zone in all calculations. Using these conditions, the lattice constants of single crystal 2H, 3C, 4H, and 6H-SiC converge to within 0.000 05 nm, and the total-energy differences among these polytypes converge to within 0.01 meV/atom. The calculated lattice constants and the total-energy difference are in good agreement with the experimental values[24,25] and previous calculations,[14,26–30] as shown in Table I.

F-terminated, OH-terminated, H-terminated, and clean 4H-SiC(0001)-1$\times$1 surfaces are modeled by a repeated slab model as shown in Fig. 1. We label the two kinds of surface structures as $4H_1$ and $4H_2$, which have cubic and hexagonal stacking sequences at the two topmost SiC bilayers, respectively.[31] In the structural optimization, the bottom four SiC bilayers and their terminating H atoms are kept fixed while all other degrees of freedom, including adsorbates, are fully relaxed. We found that the most stable adsorption site is the top site of the first layer of Si for all adsorbates. OH is inclined toward so-called H_3 site, as seen in Fig. 1. On clean surfaces, surface dangling bonds are spin polarized. A vacuum region 1.00 nm wide is inserted between two neighboring slabs and the surface energy differences converge to within 0.3 meV per 1$\times$1 unit cell for vacuum regions up to 2.00 nm wide. The work function difference between the two surfaces is compensated by a scheme proposed by Neugebauer and Scheffler.[32]

The 4H-SiC(0001) surface energy cannot be directly calculated from a slab model[33,34] because the slab model has both (0001) and $(000\bar{1})$ surfaces, and their energies cannot be calculated separately. Instead, we calculated the relative surface energy between the $4H_1$ and $4H_2$ terraces. The surface energy of the $4H_2$ terrace relative to that of the $4H_1$ terrace can be calculated by

$$\Delta E_{\text{surf}}^{4H_2} = E_{\text{surf}}^{4H_2} - E_{\text{surf}}^{4H_1} = E_{2n} - E_{2n-1} - E_{\text{bulk}}, \quad (1)$$

$$E_{\text{bulk}} = (E_{12} - E_8)/4, \quad (2)$$

where E_n is the total energy of n-layer slab and E_{bulk} is the total energy of bulk SiC per SiC pair.

Table II shows the relative $4H_2$ surface energy per 1$\times$1 surface unit cell. The relative energy converges to within 1.5 meV per 1$\times$1 unit cell by increasing the number of bilayers from 6 to 12. We found that $4H_2$ is less stable than $4H_1$ in all the cases but the relative energy depended significantly upon surface adsorbates. The surface energy difference is largest on the clean 4H-SiC(0001) surface while it is smallest on the H-terminated 4H-SiC(0001) surface. The present results strongly support the previous conclusion that the narrow and

TABLE II. The relative $4H_2$ surface energy per 1$\times$1 surface unit cell, $\Delta E_{\text{surf}}^{4H_2}$, at each terminated 4$H$-SiC(0001)-1$\times$1.

Termination	F	OH	H	Clean	ANNNI model Cal.[a]
$\Delta E_{\text{surf}}^{4H_2}$/meV	17.4	14.2	0.6	32.4	8.9

[a]Reference 10.

TABLE III. Atomic charges for F-terminated, OH-terminated, H-terminated, and clean SiC(0001)-1 $\times 1-4H_1$ surfaces.

Termination	F		OH		H		Clean	
Atomic charges			H	−0.43				
	F	−1.74	O	−1.11	H	−0.60		
	Si	2.40	Si	2.19	Si	1.27	Si	0.70
	C	−0.87	C	−0.87	C	−0.88	C	−0.91
	Si	0.89	Si	0.89	Si	0.89	Si	0.88
	C	−0.88	C	−0.88	C	−0.88	C	−0.88

broad terraces observed on wet-etched $4H$-SiC(0001)-1×1 surfaces terminated by F and OH adsorbates are $4H_2$ and $4H_1$ terraces, respectively.[12]

This termination-induced stability change in stacking sequence could be employed to control step bunching and SiC structures grown on surfaces. As seen in Table II, H termination eliminates the surface energy difference between $4H_1$ and $4H_2$. The existence of an H-terminated $4H$-SiC(0001)-1×1 surface has not yet been reported but it was reported that H-terminated $6H$-SiC(0001)-1×1 can be prepared by annealing OH-terminated $6H$-SiC(0001)-1×1 surfaces in ultrapure hydrogen at temperatures around 1000 °C.[35,36] If H-terminated $4H$-SiC(0001)-1×1 can be kept in etching or epitaxial growth processes, it may prevent the step bunching attributed to the surface energy difference.

Next, we discuss the origin of the relative stability dependence on termination. In compound semiconductors, the ionicity of atoms governs the relative stability between cubic zinc-blende and hexagonal wurtzite structures.[26] If charge asymmetry between anions and cations is large, the electrostatic attraction between anions and cations will stabilize the wurtzite structure. However, if the charge asymmetry is small, the repulsive interaction due to charge overlap will destabilize the wurtzite structure. In SiC crystal, Si and C have positive and negative charges, respectively, because of the difference in electronegativity. However, the charge asymmetry between Si and C in SiC crystal is not so large, and is close to the boundary separating the cubic zinc-blende and the hexagonal wurtzite structures.[26] Therefore, it is conceivable that if the topmost Si were more positively charged, the charge asymmetry would be enhanced and hexagonal stacking may be more stable than cubic stacking. To investigate the effect of Coulomb interaction, we estimated the atomic charges using the "fuzzy cell" method, which is an improved conventional partitioning of molecular space into so-called Voronoi polyhedra.[37] The number of electrons q_n belonging to a nucleus n is defined as

$$q_n = \int w_n(\mathbf{r})\rho(\mathbf{r})d\mathbf{r}, \tag{3}$$

where $w_n(\mathbf{r})$ is a relative weight function for each nucleus n and $\rho(\mathbf{r})$ is the density of electrons. In the fuzzy cell method, the boundaries of the polyhedra are softened and shifted from their internuclear midpoints to atomic radii-adjusted points. We determined the atomic radii of each atom from bond distances.[38]

Table III shows atomic charges for F-terminated, OH-terminated, H-terminated, and clean SiC(0001)-$1\times1-4H_1$ terraces. The atomic charges of the $4H_2$ terrace are almost the same as those of the $4H_1$ terrace and are therefore not shown. For clean and H-terminated surfaces, a simple argument based on ionicity seems to work well. A clean Si atom is less ionized than a Si atom in crystal $4H$-SiC, thus stabilizing the cubic stacking sequence as indicated in Table II. The first-layer Si of an H-terminated surface is more positively charged than that of the clean surface, leading to destabilization of the cubic stacking sequence compared with the clean surface. The first-layer Si atoms of F-terminated and OH-terminated surfaces are more positively ionized than those of H-terminated and clean surfaces. However, the cubic stacking sequence of their surfaces is more stable than that of the H-terminated surface, in strong contradiction to the ionicity argument.

To clarify the contradiction, we investigate the effect of atomic-orbital hybridization by calculating the atomic layer-resolved density of states (ALDOS). The ALDOS $D_n(k,E)$ of the nth atomic layer is defined as

$$D_n(k,E) = \int_0^a dx \int_0^b dy \int_{z_{n-1}}^{z_n} dz |\psi_{ik}(\mathbf{r})|^2 \delta(E - E_{ik}). \tag{4}$$

The boundaries z_n are placed between two neighboring atomic layers. Figure 2 shows the ALDOS of F, and the topmost Si atoms on F-terminated $4H_1$ and $4H_2$ surfaces. The most noticeable difference between the $4H_1$ and $4H_2$ terraces are the empty states near the $\bar{K}$ point. In the case of

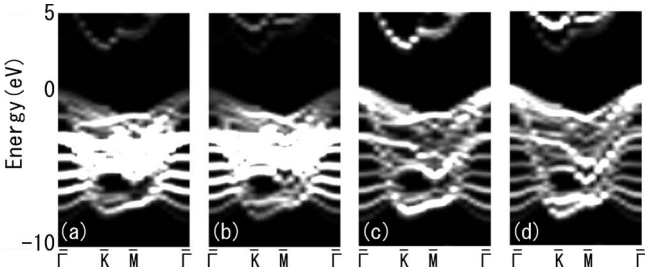

FIG. 2. ALDOS of the F atoms of (a) $4H_1$ and (b) $4H_2$, and the first-layer Si atoms of (c) $4H_1$ and (d) $4H_2$. Energy of the valence-band maximum was fixed at 0 eV.

$4H_1$ terraces, the conduction-band minima is located about 2.8 eV above the valence-band maximum (VBM), while in the $4H_2$ terraces, the weight of the conduction-band minima is quite small, and states with larger amplitude appear about 4.1 eV above the VBM. The widening of the band gap at $4H_2$ terraces is localized close to the surface and the band gaps of the bulk region of both slabs are quite similar, i.e., $\simeq 2.2$ eV. The conduction band around the minimum at the $\bar{K}$ point has large p_x and p_y characters, where x and y axes are parallel to the surface. Those empty states can hybridize occupied p_x and p_y states of F, which are located about 3.5 eV below the VBM. From the second-order perturbation theory, the energy gain due to orbital hybridization can be expressed by

$$E_{\mathrm{hyb}} = -\frac{V^2}{|E_1 - E_2|}, \tag{5}$$

where V is the matrix element between the two hybridized states, and E_1 and E_2 are the energy levels of the states. Therefore, the larger weight of the conduction-band minima at $4H_1$ terraces stabilizes the surface more than those at the $4H_2$ terraces, where the weight of the conduction-band minima is small. The energy lowering due to the hybridization of occupied p_x and p_y states with unoccupied conduction-band minima at $4H_1$ terraces is absent for H-terminated surfaces because H has no occupied p states. Although the stabilization energy is small so that we cannot easily compare the occupied F p states at the $4H_1$ terraces with the $4H_2$ terraces, we believe that the hybridization between the conduction-band minima and occupied F states is the origin of the peculiar stabilization of cubic stacking at F-terminated and OH-terminated SiC(0001)1×1 surfaces.

In conclusion, we investigated F-terminated, OH-terminated, H-terminated, and clean $4H$-SiC(0001)-1×1 surfaces using density functional theory calculations. We have shown that in all cases, the cubic stacking sequence at the top two SiC bilayers is more stable than the hexagonal stacking sequence but the energy difference between the two structures depends significantly on adsorbates. For H-terminated and clean SiC surfaces, the stability is in accordance with a simple argument based on the ionicity of surface atoms. However, the stabilization of the cubic structure at F-terminated and OH-terminated surfaces is quite peculiar, and we ascribe the effect to hybridization between the conduction-band minima, and occupied F and O states.

We acknowledge Y. Okamoto (NEC) for providing a fuzzy cell decomposition program. This research was partially supported by a grant-in-aid for JSPS Fellows 19–721 2007 and grants-in-aid for Scientific Research in Priority Areas (Development of New Quantum Simulations and Quantum Designs under Grant No. 1706400), and for 21st Century COE Program "Center for Atomistic Fabrication Technology" from the Ministry of Education, Culture, Science, Sports, and Technology, Japan. Numerical calculations were performed in the Cybermedia Center of Osaka University.

*Corresponding author; hara@up.prec.eng.osaka-u.ac.jp
†morikawa@sanken.osaka-u.ac.jp

[1] H. Matsunami, Jpn. J. Appl. Phys., Part 1 **43**, 6835 (2004).
[2] T. W. Weeks, Jr. *et al.*, Appl. Phys. Lett. **67**, 401 (1995).
[3] F. Owman, C. Hallin, P. Mårtensson, and E. Janzèn, J. Cryst. Growth **167**, 391 (1996).
[4] S. Nakamura *et al.*, Appl. Phys. Lett. **76**, 3412 (2000).
[5] H. Nakagawa, S. Tanaka, and I. Suemune, Phys. Rev. Lett. **91**, 226107 (2003).
[6] A. Nakajima, H. Yokoya, Y. Furukawa, and H. Yonezu, J. Appl. Phys. **97**, 104919 (2005).
[7] S. Soubatch *et al.*, Mater. Sci. Forum **483-485**, 761 (2005).
[8] M. Fujii and S. Tanaka, Phys. Rev. Lett. **99**, 016102 (2007).
[9] N. Ohtani *et al.*, J. Cryst. Growth **210**, 613 (2000).
[10] T. Kimoto, A. Itoh, H. Matsunami, and T. Okano, J. Appl. Phys. **81**, 3494 (1997).
[11] H. Hara *et al.*, J. Electron. Mater. **35**, L11 (2006).
[12] K. Arima *et al.*, Appl. Phys. Lett. **90**, 202106 (2007).
[13] T. Okamoto *et al.*, Mater. Sci. Forum **600-603**, 835 (2009).
[14] C. Cheng, R. J. Needs, and V. Heine, J. Phys. C **21**, 1049 (1988).
[15] V. Heine, J. Am. Ceram. Soc. **74**, 2630 (1991).
[16] F. R. Chien *et al.*, J. Mater. Res. **9**, 940 (1994).
[17] U. Lindefelt, H. Iwata, S. Öberg, and P. R. Briddon, Phys. Rev. B **67**, 155204 (2003).
[18] P. Hohenberg and W. Kohn, Phys. Rev. **136**, B864 (1964).
[19] W. Kohn and L. J. Sham, Phys. Rev. **140**, A1133 (1965).
[20] J. P. Perdew, K. Burke, and M. Ernzerhof, Phys. Rev. Lett. **77**, 3865 (1996).
[21] Y. Morikawa, Phys. Rev. B **63**, 033405 (2001).
[22] D. Vanderbilt, Phys. Rev. B **41**, 7892 (1990).
[23] N. Troullier and J. L. Martins, Phys. Rev. B **43**, 1993 (1991).
[24] A. Bauer *et al.*, Phys. Rev. B **57**, 2647 (1998).
[25] P. Villars and L. D. Calvert, *Pearson's Handbook of Crystallographic Data for Intermetallic Phases*, 2nd ed. (ASM International, Cleveland, 1991).
[26] C. H. Park, B. H. Cheong, K. H. Lee, and K. J. Chang, Phys. Rev. B **49**, 4485 (1994).
[27] P. Käckell, B. Wenzien, and F. Bechstedt, Phys. Rev. B **50**, 10761 (1994).
[28] F. Bechstedt *et al.*, Phys. Status Solidi B **202**, 35 (1997).
[29] S. Limpijumnong and W. R. L. Lambrecht, Phys. Rev. B **57**, 12017 (1998).
[30] M. C. Righi *et al.*, Phys. Rev. B **66**, 045320 (2002).
[31] The notations of $4H_1$ and $4H_2$ were used elsewhere.[10,30,12]
[32] J. Neugebauer and M. Scheffler, Phys. Rev. B **46**, 16067 (1992).
[33] J. C. Boettger, Phys. Rev. B **49**, 16798 (1994).
[34] V. Fiorentini and M. Methfessel, J. Phys.: Condens. Matter **8**, 6525 (1996).
[35] H. Tsuchida, I. Kamata, and K. Izumi, Jpn. J. Appl. Phys., Part 2 **36**, L699 (1997).
[36] T. Seyller, J. Phys.: Condens. Matter **16**, S1755 (2004).
[37] A. D. Becke, J. Chem. Phys. **88**, 2547 (1988).
[38] Si radius and C radius were determined as 1.15 and 0.75 Å, respectively. Other atomic radii were determined from each bond distance (Å): Si(1.15)-O(0.75), Si(1.15)-O(0.53), Si(1.15)-F(0.47), Si(1.15)-H(0.35), and O(0.60)-H(0.38).